Bull Eng Geol Environ (2008) 67:353–366
DOI 10.1007/s10064-008-0146-1

ORIGINAL PAPER

Estimation of strength and deformation properties of Quaternary caliche deposits

İsmail Dinçer · Altay Acar · Suphi Ural

Received: 17 September 2007 / Accepted: 28 February 2008 / Published online: 17 April 2008

Abstract The aim of this study was to develop and evaluate statistical models for predicting the uniaxial compressive strength (UCS) and average Young's modulus (E_{av}) for caliches, using some index and physical properties. The caliche samples, from Adana, southern Turkey, were of low strength and difficult to sample. X-ray diffraction and microscopy were undertaken and the following physical parameters established: unit weight, apparent porosity, Schmidt rebound number, Shore hardness, P-wave velocity, slake durability, point load, uniaxial compressive strength and average Young's modulus. Simple and linear regression variable selection analyses were performed. The best relationships were obtained for UCS with P-wave velocity and unit weight and for average Young's modulus with P-wave velocity, porosity and slake durability. Empirical equations are proposed, although it is emphasised that these may only be applicable for caliche of a similar geological character.

İ. Dinçer (✉)
Department of Technical Programs, Vocational High School,
Adıyaman University, Adıyaman 02240, Turkey
e-mail: idincer@adiyaman.edu.tr; idincer@gmail.com

A. Acar
Department of Geological Engineering,
Faculty of Engineering-Architecture,
Çukurova University, Balcalı 01330, Adana, Turkey
e-mail: iaacar@cu.edu.tr

S. Ural
Department of Mining Engineering,
Faculty of Engineering-Architecture,
Çukurova University, Balcalı 01330, Adana, Turkey
e-mail: suralp@cu.edu.tr

Keywords Hardpan · Caliche · Geomechanical properties · Index properties · Adana

Résumé Le but de cette étude est d'établir et d'évaluer des modèles statistiques permettant de prédire la résistance à la compression simple et le module d'Young de calcrètes à partir de quelques indices et propriétés physiques. Les échantillons de calcrètes d'Adana, dans le sud-est de la Turquie, présentent de faibles résistances et leur échantillonnage est difficile. Des analyses par diffractométrie RX et des observations microscopiques ont été réalisées. Les paramètres physiques suivants ont été déterminés: poids spécifique, porosité, indice de rebond de Schmidt, dureté Shore, vitesse des ondes P, indice d'altérabilité, résistance à l'écrasement entre pointes, résistance à la compression simple et module d'Young. Des analyses de régression linéaire entre ces paramètres ont été réalisées. Les meilleures relations ont été obtenues pour la résistance à la compression simple fonction de la vitesse des ondes P et du poids spécifique et pour le module d'Young fonction de la vitesse des ondes P, de la porosité et de l'indice d'altérabilité. Des équations empiriques ont été proposées, tout en soulignant que ces équations ne sauraient être utilisées que pour des calcrètes aux caractéristiques géologiques semblables.

Mots clés Calcrète d'encroûtement · Propriétés géomécaniques · Indices géotechniques · Régressions linéaires

Introduction

On the afternoon of 27 June 1998, an earthquake ($M_s = 6.3$, USGS) occurred with an epicentre located approximately 35 km southeast of Adana city, southernTurkey. The felt intensity was generally higher within low-rise buildings founded on caliche deposits. For this reason, it was considered appropriate to undertake a geomechanical study of the caliche to assist with future building construction in the Adana area.

Wright and Tucker (1991) record that the term caliche was first used to describe gravel and similar units bound by calcium carbonate in southwest America. Various authors have used the word caliche and suggested different modes of formation; e.g. leakage, capillary rise and detrital (Goudie and Pye 1983). This paper considers two major types of caliche: the upper harder material ("hardpan") with rock properties and the underlying weaker material ("softpan") with soil properties (Fig. 1a, b). Figure 1c (after Kapur et al. 1993) indicates the types of caliche found in the Adana area. Above the Handere Formation (Tertiary clay deposit), five horizons can be identified. Çobanoğlu et al. (2008) defined several types of caliche are present: the massive caliche formed of calcium carbonate (BK group), the red calciche with plant/root remains (KK group) and the calcium carbonate cemented caliche (CK).

The presence of softpan beneath the overlying harder material causes many engineering geological problems in this part of Turkey. During the motorway construction in the region, it was considered that some 90% of active and potential slides (Fig. 2a, b) were within the caliche and the colluvial deposits derived mainly from caliche (Yılmazer and Smith 1992). Many of the buildings in the area are founded on caliche and it was also used as a dimension stone in many of the historic buildings, due to its capability of being shaped easily (Fig. 2c, d). In some parts of the world where the caliche is stronger, it forms excellent road paving material (Horta 1980). As the caliche in the Adana area has only low strength (range 2.03–10.41 MPa), it is difficult to prepare for standard testing.

Many researchers reported that the uniaxial compressive strength and Young's modulus of rock are important parameters to explain the strength and deformation characteristics of rocks (Bieniawski 1974). However, the literature indicates that there is no single relationship, which applies to all rock types, by which the strength and Young's modulus can be estimated from rock index tests (e.g. Miller 1965; Deere and Miller 1966; Aufmuth 1973; Beverly et al. 1979; Kindybinski 1980; Singh et al. 1983; Shorey et al. 1984; Haramy and De Marco 1985; Ghose and Chakrabarti 1986; O'Rourke 1989; Sachpazis 1990; Xu et al. 1990; Gökçeoğlu 1996; Aggistalis et al. 1996; Kahraman 1996; Koncagül and Santi 1999; Katz et al. 2000; Yılmaz and Sendir 2002; Yaşar and Erdoğan 2004a; Yaşar and Erdoğan 2004b; Karakuş et al. 2004; Kahraman 2001; Dinçer et al. 2004).

This study was undertaken to develop and evaluate statistical models for predicting uniaxial compressive strength (UCS) and average Young's Modulus (E_{av}) of the caliche deposits which outcrop in the Adana area, southern Turkey, between Lat 36.80°–37.50°N and Long 34.50°–35.50°E (Fig. 3).

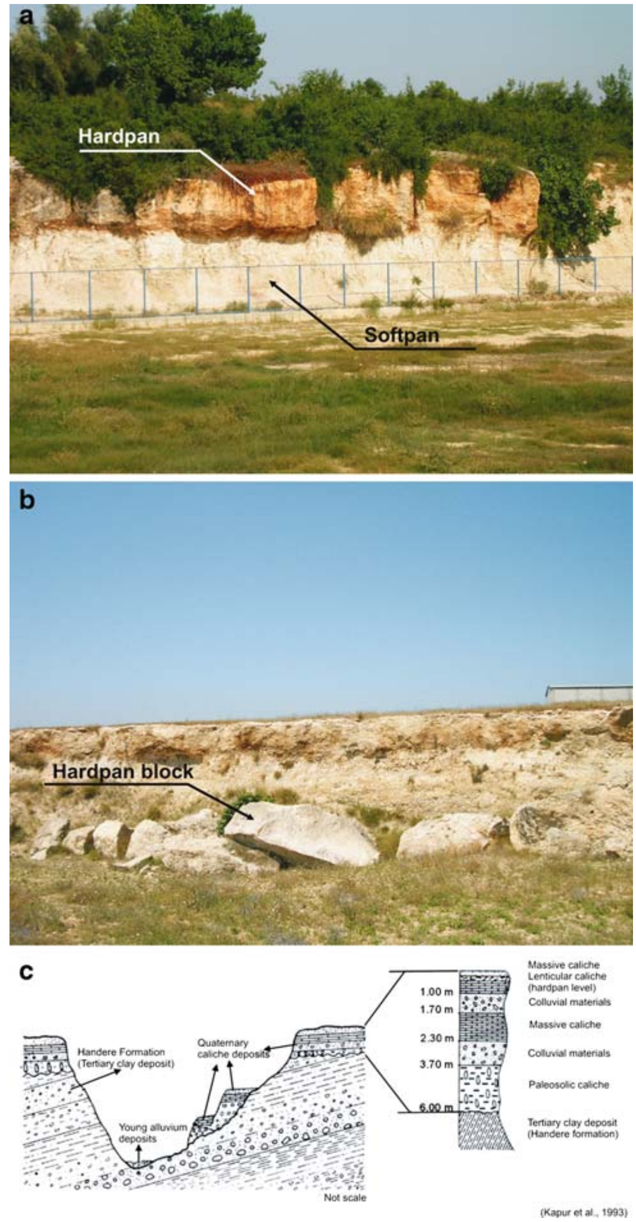

Fig. 1 Various views of the caliche outcrops and samples: **a** hardpan level of caliche, **b** large hardpan blocks, **c** general cross and stratigraphic section of caliche in the study area

Mineralogy

Mineralogical analyses were carried out to determine the type and percentage of minerals in the caliche samples using X-ray diffraction (XRD). Diffractograms of the

Fig. 2 **a** Motorway slope failure in caliche deposits, **b** mass movement in caliche deposits, triggered by 1998 Adana–Ceyhan earthquake, (**c**, **d**) the use of caliche hardpan as a dimension stone

caliche samples were obtained at the laboratories of the Metallurgical and Materials Department of Anadolu University using a Rigaku diffractometer system with Cu Kα radiation. Samples were run from 5° to 70° 2θ with a step increment of 0.02° and counting time of 2 s/step; the relevant data were stored in a digital form. Thin sections were prepared to examine the mineralogy of both grains and bonding material and the average size and shape of the grains and pores of the caliche samples.

Mechanical tests

Rock block samples (approximately 0.25 × 0.25 × 0.20 m) were collected from the hardpan in 19 different locations (Fig. 3) and NX and BX sized cores prepared (Fig. 4a, b). Unit weight (UW), apparent porosity (n), Schmidt rebound number (R_N), Shore hardness (SH), P-wave velocity (V_p), slake durability index (I_{d2}), point load index ($Is_{(50)}$), UCS and average Young's Modulus (E_{av}) values were obtained following ISRM (1981a).

Rock samples with a regular shape were used for the unit weight and apparent porosity tests. The samples were submerged in water for 48 h and weight/dimensions measured to an accuracy of ±0.01. After drying for 24 h at 105°C the samples were again weighed and apparent porosity and unit weight established.

The Schmidt hammer tests were carried out in the field on large caliche block samples using an N type hammer following (ISRM 1981b). The Schmidt hammer tests were performed vertically on rock blocks with no visible discontinuities. Each test involved twenty readings, with the upper ten values averaged to give the final result.

Shore hardness values were determined using the C2 type Shore scleroscope. The test involved dropping a 2.44 g diamond-tipped hammer freely onto the caliche sample and carefully measuring the rebound height. Again 20 readings were taken from each sample; the highest and lowest 5 being discarded and the remaining 10 averaged following ISRM (1978a).

For the P-wave velocity test, three core samples were prepared (height/diameter 2–2.5) for each caliche. Both faces of drill cores were trimmed and smoothed so that the receiver and the transmitter could cover the faces tightly. The test was carried out according to ISRM (1978b).

The slake durability testing was undertaken following ISRM (1979) using a ELE RM-310-2 test machine. Ten rock lumps with equal dimensions were rotated in the steel mesh drum, partially immersed in water for ten minutes. Samples were subjected to three cycles and the durability index (I_d) in each cycle was calculated as a percentage ratio

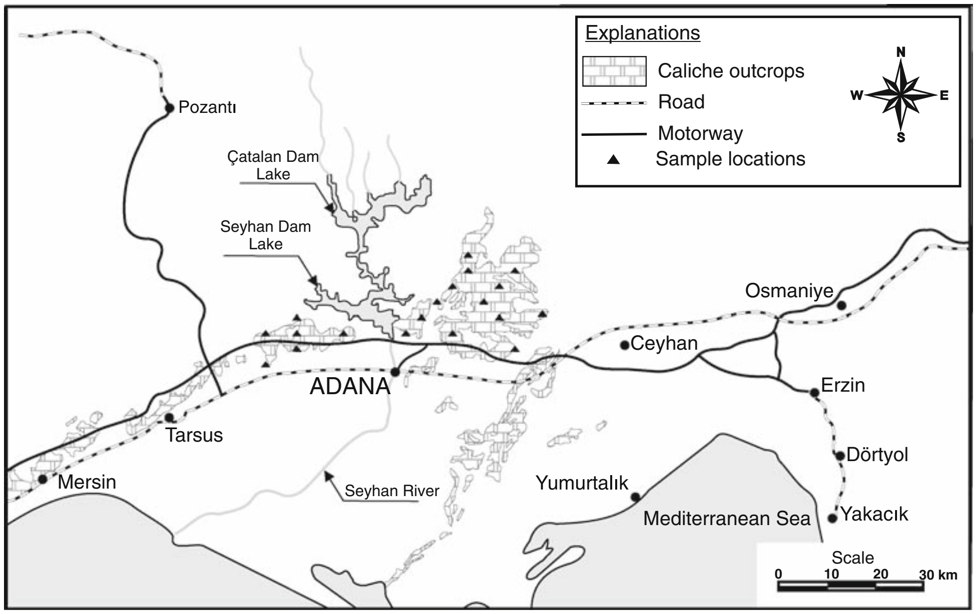

Fig. 3 Location of the study area

Fig. 4 **a** Cored caliche blocks, **b** NX and BX size caliche core samples

of final to initial dry weight of rocks in the drum after the drying and wetting cycles. In this study, the second cycle index (I_{d2}) was used for the evaluation of the slake durability index of the caliche.

In this study diametrical and axial point load tests were undertaken according to ISRM (1985) on core samples with a length/diameter ratio of 1:1. Failure of rock samples was achieved within 10–60 s. The point load strength index $Is_{(50)}$ was calculated using the correction factor.

The uniaxial compressive strength tests were performed according to ISRM (1981c) using an ELE ADR 2000 machine and a data acquisition system. NX and BX size core samples (length/diameter 2–2.5) were prepared. The loading rate was 0.1 kN/s and failure of the caliche samples was achieved within 5–10 min. At least five specimens were tested for each block sample.

Young's modulus (E_{av}) was established following the ISRM (1981c) standard test procedure.

Principal component and regression analysis

The UCS and average Young's modulus of the caliche samples were correlated with their index properties using simple stepwise multiple regression techniques including *F*-tests. For the analysis of several variables, adapted multivariate statistical methods were employed. The principal component analysis (PCA) is among the best known of these methods. Its objective is to describe the dependence structure observed in the dataset through latent factors which are fewer in number than the original variables. These derived factors are essentially linear combinations of the original variables (Davis 1986).

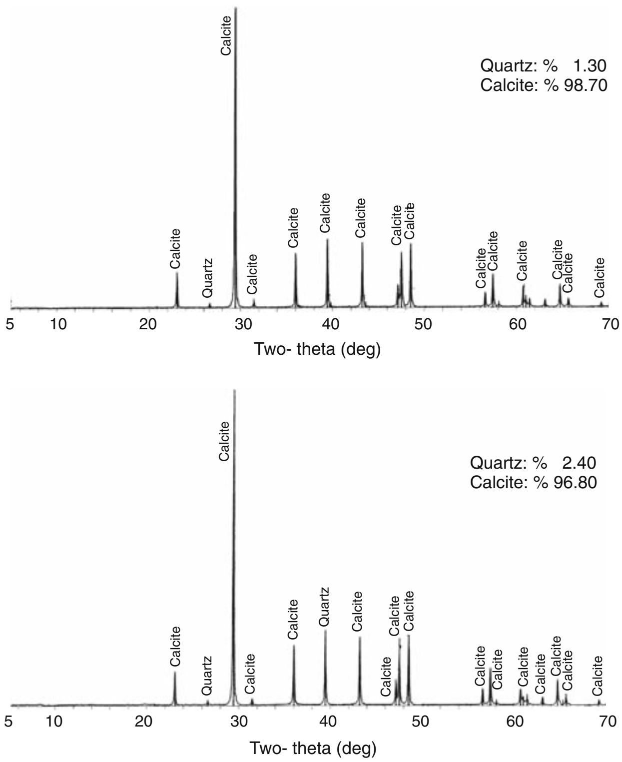

Fig. 5 Selected XRD patterns for hardpan (caliche) samples

A stepwise forward selection procedure was used to select the best suitable regression model.

Mineralogical and physico-chemical properties

Strength and slaking are among the engineering properties influenced by the physico-chemical characteristics of a rock (e.g. Fahy et al. 1979; Shakoor and Bonelli 1991; Gunsallus and Kulhawy 1984; Koncagül and Santi 1999). In order to determine the physico-chemical properties of the caliche, both XRD and thin section analyses were undertaken.

As seen from Fig. 5, the diffractograms indicate in excess of 96.80% calcite with quartz accounting for some 1.30–3.00%.

Macroscopically, the colour of the massive caliche was determined as 10YR 8/2, 5YR 5/6, 5YR 8/6, 10YR 7/4, 10YR 8/6 and 10YR 5/4.

All of the thin sections contained elongated, irregularly dispersed, thin rootlets and calcite crystals. The groundmass is a dark micrite with rare microsparite in the voids and nodules (Fig. 6a, b). In some samples, the voids were infilled with microsparite and sparite with a serrated boundary. Very dense nodules are dark greyish white in colour and their ground mass microcrystalline and irregular in shape. Vughs with rough undulations were observed, which may result from the voids being enlarged during the

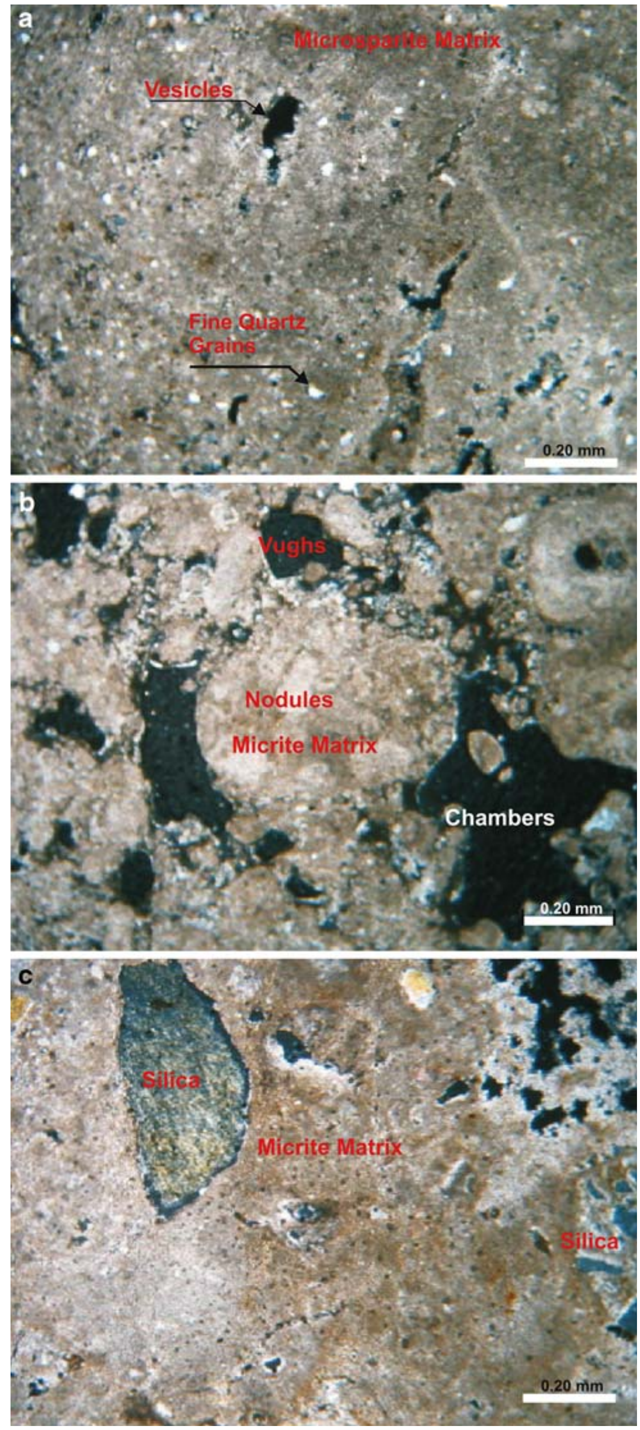

Fig. 6 Thin section views of hardpan (caliche) samples

preparation of the thin section. Silt sized quartz grains were abundant in the microcrystalline calcite (Fig. 6a). Angular and sub-angular and moderately well sorted limestone gravels were seen in all the thin sections and some samples also contained silica, marble, siltstone, sandstone and re-crystallized limestones, generally in the caliche above the river terrace deposits (Fig. 6c).

Table 1 Laboratory test results for the 19 caliche samples

Sample no.	Unit weight (kN/m^3)	Schmidt rebound number (R_N)	Shore hardness (SH)	P-wave velocity V_p (m/sn)	Apparent porosity n (%)	Slake durability index (two cycles) I_{d2} (%)	Point load index $Is_{(50)}$ MPa	Uniaxial compressive strength, UCS (MPa)	Average Young's modulus E_{av} (GPa)
BL-1	18.51	28.00	13.54	681	28.12	90.08	1.13	5.63	0.55
BL-2	17.93	24.60	8.58	491	28.44	94.29	0.97	3.37	0.19
BL-3	21.55	27.80	12.13	1,146	21.00	97.53	1.25	7.85	0.88
BL-4	14.96	14.50	4.20	375	34.79	65.36	0.53	2.03	0.16
BL-5	19.17	31.40	12.04	509	23.98	92.76	0.96	4.52	0.52
BL-6	18.70	35.40	18.08	1,085	26.36	96.92	1.69	6.28	0.68
BL-7	17.32	19.90	8.40	436	31.70	84.82	0.78	2.99	0.19
BL-8	20.33	26.90	11.00	758	24.15	90.52	1.03	6.50	0.82
BL-9	19.84	26.00	11.80	727	23.75	93.52	0.97	4.90	0.63
BL-11	18.87	22.00	9.60	713	26.73	90.15	0.79	4.32	0.59
BL-12	22.00	39.80	22.50	1,444	16.23	96.81	1.91	9.54	1.29
BL-13	18.26	27.50	11.46	477	26.23	91.90	0.86	2.65	0.18
BL-14	19.16	28.98	14.01	705	23.50	93.23	1.17	5.83	0.57
BL-15	19.45	26.69	9.31	533	30.86	85.00	1.05	3.65	0.21
BL-16	21.77	30.30	13.22	1,249	22.00	98.00	1.72	8.55	0.95
BL-18	20.20	33.08	12.68	537	25.26	86.20	1.01	4.76	0.54
BL-19	19.51	36.94	18.87	1,132	24.60	98.34	1.58	6.56	0.70
BL-20	17.75	20.40	8.61	446	32.49	86.94	0.80	3.06	0.21
BL-21	22.94	43.44	24.56	1,576	17.71	98.10	2.08	10.41	1.40

Physico-mechanical properties

The physico-mechanical properties of the caliche are given in Table 1. It can be seen that the unit weight varied from 14.96 to 22.94 kN/m^3, similar to the value (17.46 kN/m^3) reported by Zorlu and Kasapoğlu (2004). Apparent porosity (n) ranged from 16.23 to 34.79%. According to IAEG (1979), all the caliche samples classify as of medium-high porosity.

The Schmidt rebound values (R_N) ranged between 14.50 and 43.44 while the Shore hardness (SH) values were between 4.20 and 24.56. The point load index ($Is_{(50)}$) varied from 0.53 to 2.08 MPa, ie the caliche is a low-very low strength rock according to Bieniawski (1974). The UCS ranged between 2.03 and 10.41 MPa. The average Young's modulus (E_{av}) varied from 0.16 to 1.40 GPa.

The highest P-wave velocity (V_p) was 1,576 m/s and the lowest 375 m/s. The slake durability test results (I_{d2}) ranged from 65.36 to 98.34%.

Data analyses

The first phase of the analysis considered the relationship between the UCS and the index tests. The correlation circle on the factorial plane (Fig. 7a) determined by the first two principal components indicated that the UCS was positively correlated with the V_p, UW, $Is_{(50)}$, SH and R_N, but negatively correlated with the porosity (n). In addition, a slight positive correlation could be discerned between the UCS and I_{d2}. The UCS and the Young's modulus (E_{av}) were also analysed; Fig. 7b shows the correlation circle determined by the first two principal components and the projection of the various vectors representing the variables studied. It can be seen the arrangement of the vectors is similar to that shown in Fig. 7a.

Prediction of the mechanical properties of caliche

In order to be able to describe the relationships between compressive strength (UCS) and average Young's modulus (E_{av}) and the index and physical properties of the tested caliche samples, simple regression analysis was undertaken based on linear, logarithmic, power and exponential laws using the data set given in Table 1. Regression analysis was performed using SPSS for Windows statistical software. The results are shown in Fig. 8 and the regression equations are presented in Table 2. Only P-wave velocity (V_p) has a statistically significant correlation with UCS and

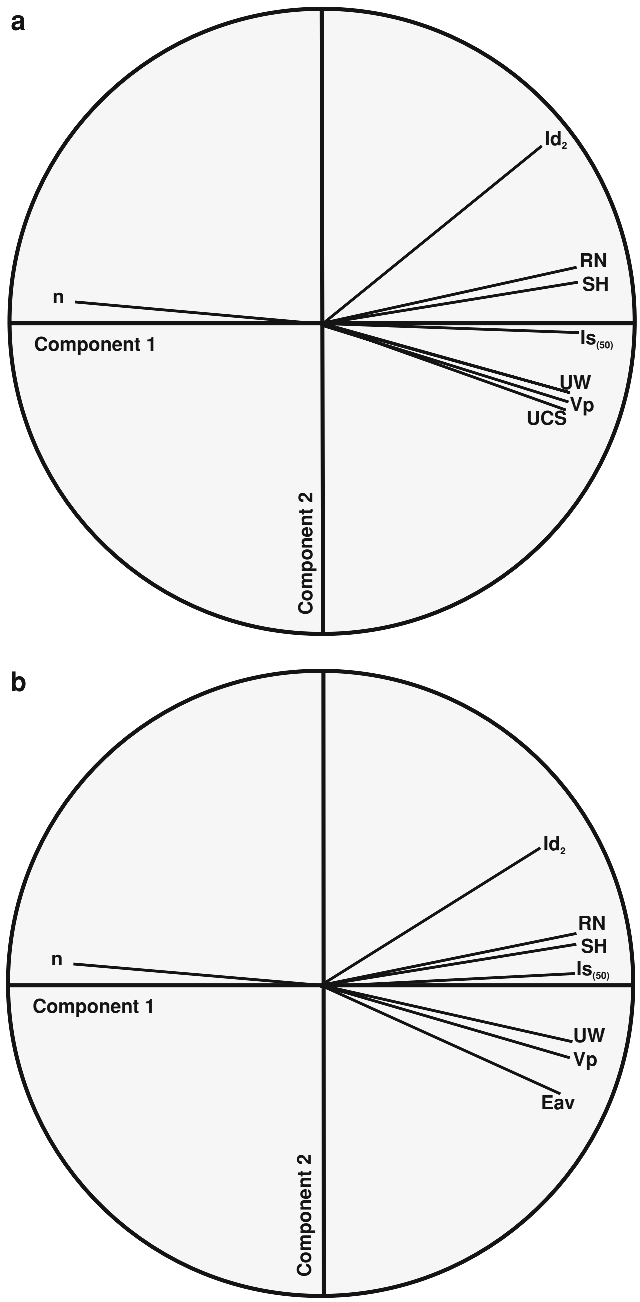

Fig. 7 PCA correlation circles **a** influence of the geometrical parameters on the UCS, **b** influence of the geometrical parameters on the E_{av}. (*n* apparent porosity, V_p P wave velocity, *UW* unit weight, $Is_{(50)}$ point load index, *SH* shore hardness, R_N Schmidt rebound number, I_{d2} slake durability index, *UCS* uniaxial compressive strength, E_{av} average Young's modulus)

E_{av}, with regression coefficients (R^2) of 0.91 and 0.87, respectively.

Multiple linear regression analyses were considered to derive equations that could be used to predict UCS and average Young's modulus (E_{av}) from the index and physical properties of the caliche.

For UCS, the best model found was:

$$\mathrm{UCS} = -6.319 + 4.418 \times 10^{-3}\mathrm{Vp} + 0.427\mathrm{UW}. \quad (1)$$

The *F* test indicated:

$$F_{\text{Calculated}} = 157.926 \text{ and } F_{[\alpha]}^{(k-1,n-k)} = F_{[0.050]}^{(3-1,19-3)} = F_{[0.050]}^{(2,16)} = 3.63$$

$$F_{\text{Calculated}} > F_{[0.050]}^{(2,16)} = 157.926 > 3.63$$

As seen from Table 3, all the absolute *t* values were greater than the *t* table values and all the VIF values are less than 10. The adjusted R^2 value (94.6% with a standard deviation of 0.553) indicates that the above multiple regression model was appropriate for calculating the total variation in the 19 UCS tests. The stepwise forward technique for regression analysis revealed P-wave velocity (V_p) to be the most important variable, followed by unit weight.

Measured and predicted values of UCS were compared; the linear regression line was plotted, together with the equation for the regression line ($y = ax + b$) and the relevant correlation coefficient. A diagonal line was drawn on each graph, representing the line along which the points would fall if the proportions of the estimated data were exactly equal to the measured data. As can be seen in Fig. 9, a good prediction was achieved using the proposed model with the points plotting very close to the diagonal line. The regression equation has a slope very similar to the 1:1 line, indicating a high correlation coefficient (R^2 = 0.95) and low intercept value.

A regression model was also developed to predict average Young's modulus (E_{av}) using apparent porosity (*n*), Schmidt rebound values (R_N), Shore hardness (SH), P-wave velocity (V_p), slake durability (I_{d2}), unit weight (UW) and point load index ($Is_{(50)}$). Figures 10 and 11 show the correlations obtained using Tables 4 and 5 and the following equations:

$$E_{av} = 0.944 + 5.899 \times 10^{-4}V_p - 3.17 \times 10^{-2}n \quad (2)$$

$$E_{av} = 2.201 + 6.224 \times 10^{-4}V_p - 4.30 \times 10^{-2}n - 1.09 \times 10^{-2}I_{d2} \quad (3)$$

The *F* tests indicated:

$$F_{\text{Calculated}} = 104.565 \text{ and } F_{[\alpha]}^{(k-1,n-k)} = F_{[0.050]}^{(3-1,19-3)} = F_{[0.050]}^{(2,16)} = 3.63$$

$$F_{\text{Calculated}} > F_{[0.050]}^{(2,16)} = 104.565 > 3.63$$

for Eq. (2) and,

$$F_{\text{Calculated}} = 96.039 \text{ and } F_{[\alpha]}^{(k-1,n-k)} = F_{[0.050]}^{(4-1,19-4)} = F_{[0.050]}^{(3,15)} = 3.29$$

$$F_{\text{Calculated}} > F_{[0.050]}^{(3,15)} = 96.039 > 3.63$$

for Eq. (3).

Table 2 Simple regression model and ANOVA for dependent variables (UCS and E_{av})

Source	Type of model	R^2	Adjusted R^2	Std. error of the estimate	Mean square		df		F	Sig.F	Equation
					Regression	Residual	Regression	Residual			
UCS–UW	Linear	0.794	0.782	1.111	80.718	1.233	1	17	65.444	0.000	$UCS = 1.131UW - 16.471$
	Logarithmic	0.761	0.747	1.196	77.357	1.431	1	17	54.053	0.000	$UCS = 21.035Ln(UW) - 56.81$
	Power	0.800	0.788	0.208	2.951	0.043	1	17	68.075	0.000	$UCS = 2.60 \times 10^{-5} UW^{4.108}$
	Exponential	0.807	0.796	0.205	2.976	0.711	1	17	71.164	0.000	$UCS = 0.0737e^{0.217UW}$
UCS–RN	Linear	0.640	0.618	1.468	65.037	2.156	1	17	30.169	0.000	$UCS = 0.267RN - 2.210$
	Logarithmic	0.600	0.579	1.547	61.005	2.393	1	17	25.493	0.000	$UCS = 7.044Ln(RN) - 17.96$
	Power	0.659	0.539	0.272	2.431	0.074	1	17	32.914	0.000	$UCS = 4.6 \times 10^{-2} RN^{1.406}$
	Exponential	0.649	0.628	0.276	2.391	0.076	1	17	31.368	0.000	$UCS = 1.143e^{0.051RN}$
UCS-SH	Linear	0.709	0.692	1.320	72.062	1.743	1	17	41.354	0.000	$UCS = 0.397SH + 0.332$
	Logarithmic	0.667	0.648	1.411	67.838	1.991	1	17	34.071	0.000	$UCS = 4.830Ln(SH) - 6.546$
	Power	0.722	0.706	0.245	2.664	0.060	1	17	44.249	0.000	$UCS = 0.461SH^{0.957}$
	Exponential	0.675	0.656	0.266	2.488	0.071	1	17	35.278	0.000	$UCS = 1.918e^{0.074SH}$
UCS–Vp	Linear	0.913	0.908	0.720	92.884	0.518	1	17	179.391	0.000	$UCS = 6 \times 10^{-3} V_p - 0.556$
	Logarithmic	0.913	0.908	0.722	92.813	0.522	1	17	177.823	0.000	$UCS = 5.136Ln(V_p) - 28.337$
	Power	0.885	0.879	0.158	3.264	0.025	1	17	131.179	0.000	$UCS = 9 \times 10^{-3} V_p^{0.963}$
	Exponential	0.818	0.808	0.198	3.018	0.039	1	17	76.597	0.000	$UCS = 2.054e^{0.001V_p}$
UCS–n	Linear	0.780	0.767	1.148	79.278	1.318	1	17	60.146	0.000	$UCS = -0.439n + 16.717$
	Logarithmic	0.802	0.790	1.088	81.552	1.184	1	17	68.860	0.000	$UCS = -10.960Ln(n) - 40.826$
	Power	0.756	0.742	0.230	2.788	0.053	1	17	52.706	0.000	$UCS = 3439.38n^{-2.02}$
	Exponential	0.774	0.761	0.221	2.855	0.049	1	17	58.289	0.000	$UCS = 42.111e^{-0.083n}$
UCS–I_{d2}	Linear	0.468	0.436	1.785	47.548	3.185	1	17	14.931	0.001	$UCS = 0.211I_{d2} - 13.815$
	Logarithmic	0.427	0.394	1.851	43.455	3.425	1	17	12.686	0.002	$UCS = 16.636Ln(I_{d2}) - 69.552$
	Power	0.545	0.518	0.314	2.010	0.099	1	17	20.376	0.000	$UCS = 4.9 \times 10^{-7} I_{d2}^{3.578}$
	Exponential	0.577	0.552	0.303	2.127	0.092	1	17	23.161	0.000	$UCS = 0.084e^{0.45I_{d2}}$
UCS-$Is_{(50)}$	Linear	0.829	0.819	1.011	84.322	1.021	1	17	82.559	0.000	$UCS = 5.096Is_{(50)} - 0.533$
	Logarithmic	0.814	0.803	1.055	82.767	1.113	1	17	74.372	0.000	$UCS = 6.088Ln(Is_{(50)}) + 4.833$
	Power	0.817	0.807	0.199	3.014	0.040	1	17	76.092	0.000	$UCS = 4.413Is_{(50)}^{1.162}$
	Exponential	0.765	0.751	0.226	2.821	0.051	1	17	55.347	0.000	$UCS = 1.662e^{0.932Is_{(50)}}$
E_{av}–UW	Linear	0.767	0.754	0.181	1.841	0.033	1	17	56.092	0.000	$E_{av} = 0.171UW - 2.713$
	Logarithmic	0.729	0.713	0.196	1.749	0.038	1	17	45.743	0.000	$E_{av} = 3.163Ln(UW) - 8.766$
	Power	0.720	0.703	0.377	6.204	0.142	1	17	43.642	0.000	$E_{av} = 1.07 \times 10^{-8} UW^{5.957}$
	Exponential	0.729	0.714	0.370	6.288	0.137	1	17	45.827	0.000	$E_{av} = 1 \times 10^{-3} e^{0.316UW}$

Table 2 continued

Source	Type of model	R^2	Adjusted R^2	Std. error of the estimate	Mean square		df		F	Sig.F	Equation
					Regression	Residual	Regression	Residual			
E_{av}–RN	Linear	0.607	0.584	0.235	1.457	0.055	1	17	26.284	0.000	$E_{av} = 0.040RN - 0.549$
	Logarithmic	0.548	0.521	0.253	1.315	0.064	1	17	20.612	0.000	$E_{av} = 1.034Ln(RN) - 2.840$
	Power	0.570	0.545	0.467	4.914	0.218	1	17	22.540	0.000	$E_{av} = 6.3 \times 10^{-4} RN^{1.999}$
	Exponential	0.573	0.548	0.465	4.943	0.216	1	17	22.854	0.000	$E_{av} = 0.059e^{0.074RN}$
E_{av}–SH	Linear	0.695	0.677	0.207	1.668	0.043	1	17	38.758	0.000	$Eav = 0.060SH - 0.181$
	Logarithmic	0.624	0.601	0.230	1.496	0.053	1	17	28.164	0.000	$Eav = 0.717Ln(SH) - 1.184$
	Power	0.643	0.622	0.426	5.542	0.181	1	17	30.599	0.000	$E_{av} = 0.016SH^{1.380}$
	Exponential	0.612	0.589	0.444	5.272	0.197	1	17	26.767	0.000	$E_{av} = 0.122e^{0.107SH}$
E_{av}–n	Linear	0.814	0.803	0.162	1.954	0.026	1	17	74.593	0.000	$E_{av} = -0.069n + 2.367$
	Logarithmic	0.846	0.837	0.147	2.030	0.022	1	17	93.491	0.000	$E_{av} = -1.729Ln(n) + 6.179$
	Power	0.759	0.745	0.350	6.543	0.122	1	17	53.554	0.000	$E_{av} = 10952.07n^{-3.104}$
	Exponential	0.785	0.772	0.331	6.763	0.109	1	17	61.906	0.000	$E_{av} = 13.092e^{-0.128n}$
E_{av}–V_p	Linear	0.873	0.865	0.134	2.094	0.018	1	17	116.729	0.000	$E_{av} = 1 \times 10^{-3} V_p - 0.137$
	Logarithmic	0.861	0.854	0.140	2.068	0.019	1	17	106.217	0.000	$E_{av} = 0.767Ln(V_p) - 4.446$
	Power	0.816	0.805	0.305	7.035	0.093	1	17	75.471	0.000	$E_{av} = 4.44 \times 10^{-5} V_p^{1.414}$
	Exponential	0.739	0.724	0.364	6.372	0.132	1	17	48.193	0.000	$E_{av} = 0.135e^{0.002V_p}$
E_{av}–I_{d2}	Linear	0.387	0.351	0.294	0.929	0.087	1	17	10.738	0.005	$E_{av} = 0.030I_{d2}$-2.095
	Logarithmic	0.351	0.313	0.303	0.841	0.092	1	17	9.182	0.008	$E_{av} = 2.315Ln(I_{d2}) - 9.840$
	Power	0.432	0.399	0.536	3.728	0.288	1	17	12.952	0.003	$E_{av} = 1.4 \times 10^{-10} I_{d2}^{4.873}$
	Exponential	0.462	0.431	0.522	3.986	0.273	1	17	14.620	0.002	$E_{av} = 0.002e^{0.061I_{d2}}$
$E_{av} - Is_{(50)}$	Linear	0.730	0.714	0.195	1.752	0.038	1	17	45.965	0.000	$E_{av} = 0.734Is_{(50)} - 0.265$
	Logarithmic	0.686	0.668	0.210	1.647	0.044	1	17	37.213	0.000	$E_{av} = 0.859Ln(Is_{(50)}) + 0.510$
	Power	0.639	0.617	0.428	5.505	0.183	1	17	30.038	0.000	$E_{av} = 0.416Is_{(50)}^{1.570}$
	Exponential	0.612	0.590	0.443	5.279	0.197	1	17	30.038	0.000	$E_{av} = 0.109e^{1.275Is_{(50)}}$

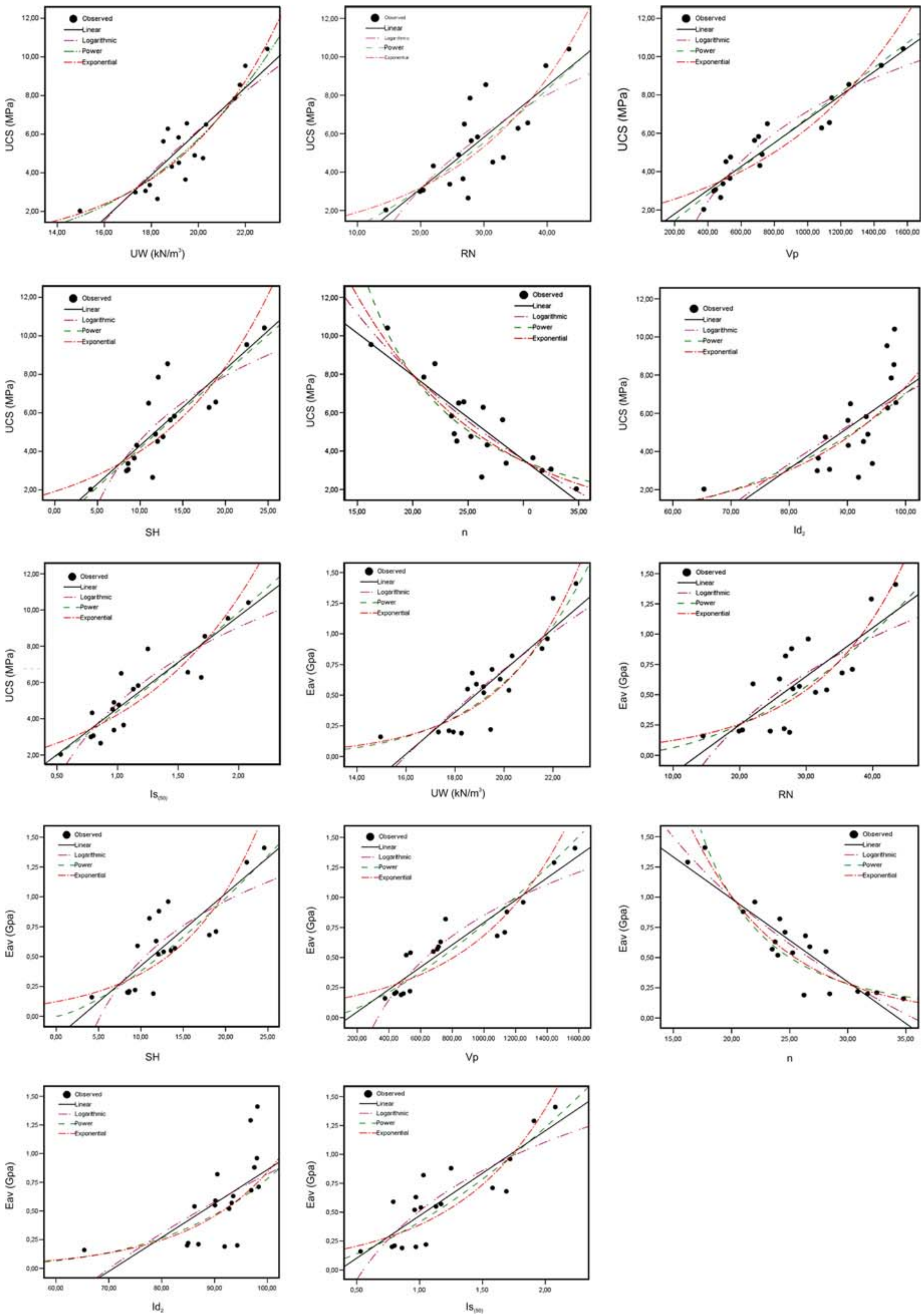

Fig. 8 The relationship between uniaxial compressive strength, average Young's modulus and index and physical properties of hardpan (caliche) samples

Table 3 Relationship between UCS and V_p and UW

Independent variables	Unstandardised coefficients		t	Sig.	Variance inflation factor (VIF)
	β	Std. error			
Constant	−6.319	1.950	−3.241	0.005	
V_p	4.418×10^{-3}	0.001	7.249	0.000	2.942
UW	0.427	0.120	3.570	0.003	2.942

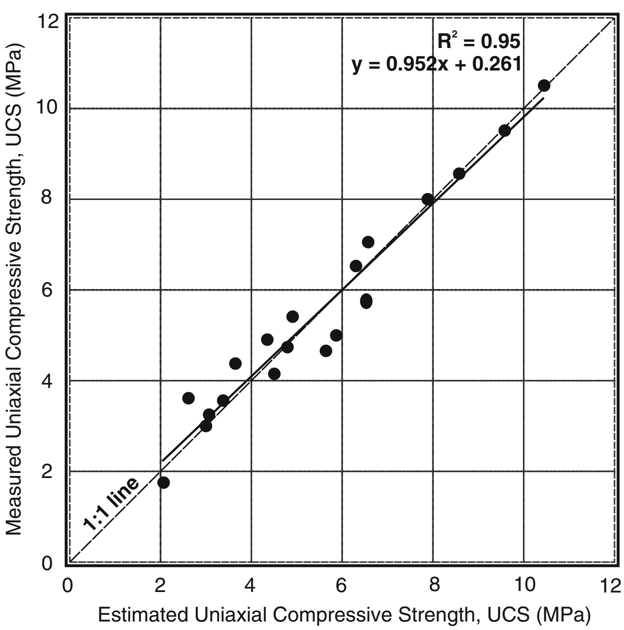

Fig. 9 Comparison of measured and the estimated UCS values for Eq. (1)

Again, all the absolute t values are greater than the t table values and all the VIF values are smaller than 10. Figures 10 and 11 support a linear relationship between the average Young's modulus (E_{av}) P-wave velocity (V_p), apparent porosity (n) and slake durability (I_{d2}), with regression equation slopes equal to 1.0, a high correlation coefficient (R^2 above 0.93) and very low intercept values.

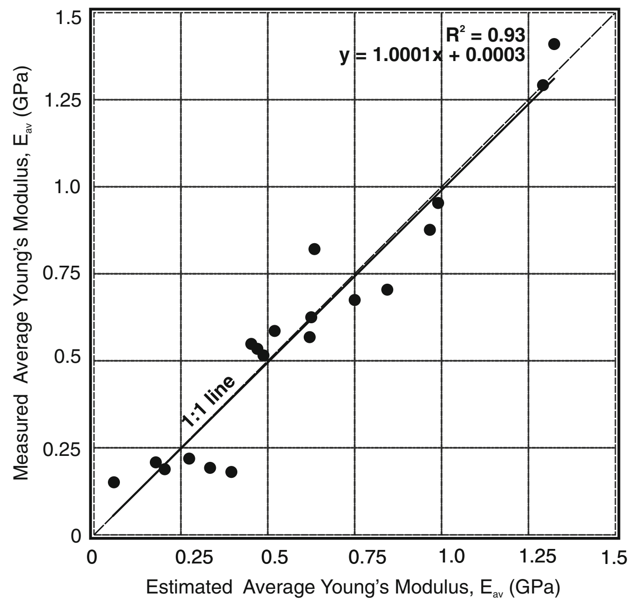

Fig. 10 Comparison of measured and the estimated E_{av} values for Eq. (2)

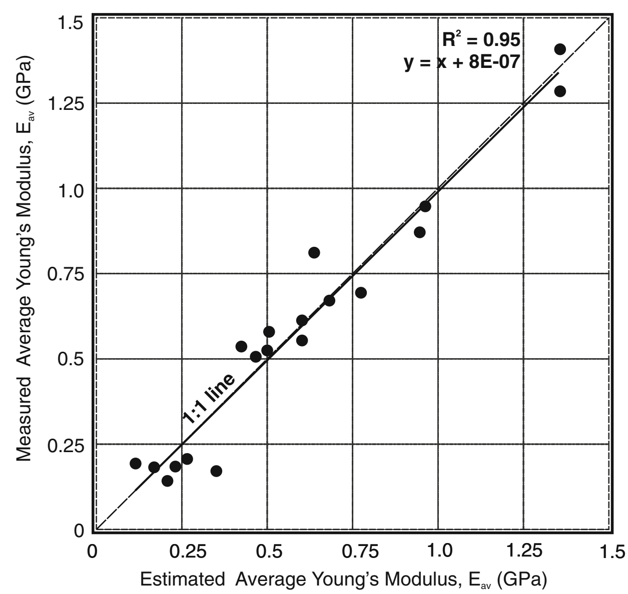

Fig. 11 Comparison of measured and the estimated E_{av} values for Eq. (3)

Discussion

Simple and multiple linear regression analyses were performed to estimate both the UCS and average Young's modulus (E_{av}) of caliche. More than fifty simple equations were performed using index and physical properties and evaluated by statistical regression analysis. There is a good statistical relationship between the UCS and E_{av} of the caliche studied. The models suggest that E_{av} is best estimated by P-wave velocity, apparent porosity (n) and slake durability (I_{d2}). The UCS is a function of P-wave velocity (V_p) and unit weight (UW).

These models have excluded the Schmidt rebound values (R_N), Shore hardness (SH), and point load index ($Is_{(50)}$). The application of the Schmidt hammer test on very soft and extremely hard rocks is not recommended (Xu et al. 1990) and it is difficult to prepare smooth test surfaces on which the measurements are taken. In the same way, using point load strength test on caliche is quite

Table 4 Relationship between E_{av} and V_p, n and I_{d2}

Independent variables	Unstandardised coefficients		t	Sig.	Variance inflation factor (VIF)
	β	Std. error			
Constant	0.944	0.310	3.047	0.008	
V_p	5.899×10^{-4}	0.000	5.079	0.000	3.073
n	-3.17×10^{-2}	0.009	−3.552	0.003	3.073
Constant	2.201	0.559	3.939	0.001	
V_p	6.224×10^{-4}	0.000	6.169	0.000	3.123
N	-4.30×10^{-2}	0.009	−4.848	0.000	4.089
I_{d2}	-1.09×10^{-2}	0.004	−2.558	0.022	2.434

Table 5 Correlation coefficient for E_{av}

R	R^2	Adjusted R^2	Standard error of the estimate
0.964[a]	0.929	0.920	0.103
0.975[b]	0.951	0.941	0.088

[a] Predictors: (Constant), V_p, n

[b] Predictors: (Constant), V_p, n, I_{d2}

problematic because of the penetration of the points into the sample. For this reason, the point load index is not a good predictor for estimating the UCS and averages Young's modulus (E_{av}) of caliche. Shore hardness test are also known to be more reliable for strong rocks.

The study has shown that the uniaxial strength of the Adana caliche can be estimated from P-wave velocity (V_p) and unit weight (UW), using the proposed empirical relationship $UCS = -6.319 + 4.418 \times 10^{-3} V_p + 0.427UW$. Two different empirical equations were proposed for the estimation of average Young's modulus (E_{av}) using P-wave velocity (V_p), apparent porosity (n) and slake durability (I_{d2}): $E_{av} = 0.944 + 5.899 \times 10^{-4}\ V_p - 3.17 \times 10^{-2} n$ and $E_{av} = 2.201 + 6.244 \times 10^{-4}\ V_p - 4.30 \times 10^{-2}\ n - 1.09 \times 10^{-3}\ I_{d2}$. These models have very high correlation coefficients (R^2) of 0.946 (for Eq. 1), 0.920 (for Eq. 2), and 0.941 (for Eq. 3).

The best relationships were obtained for P-wave velocity, which is a non-destructive test and easy to apply in both site and laboratory conditions. In rock engineering, sound velocity techniques have increasingly been used to determine the dynamic properties of rocks. The measured and predicted values for the 19 samples detailed in Table 1 are shown in Fig. 12 for UCS and V_p (Eq. 1) and Fig. 13 for average Young's modulus and V_p and porosity (Eq. 2) and V_p, porosity and slake durability (Eq. 3). The empirical equations obtained using Schmidt rebound values (R_N), Shore hardness (SH), and point load index ($Is_{(50)}$) yielded results very different from the measured values.

Conclusions

The aim of this research was to establish empirical equations for estimating the uniaxial compressive strength and average Young's modulus of caliches from Adana using unit weight (UW), apparent porosity (n), Schmidt rebound values (R_N), Shore hardness (SH), slake durability (I_{d2}), P-wave velocity (V_p) and point load index ($Is_{(50)}$). Shore hardness, Schmidt rebound numbers and point load index were not found to be good predictors; these parameters are known to have greater validity for the testing of strong rocks.

The model with P-wave velocity, using the proposed empirical equations of $UCS = -6.319 + 4.418 \times 10^{-3}$

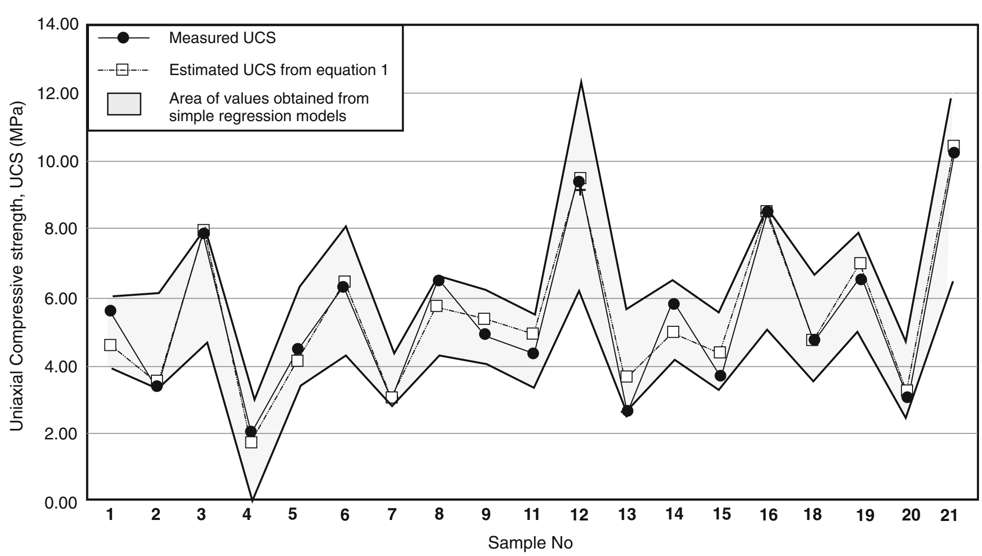

Fig. 12 Comparison of measured and estimated values of the uniaxial compressive strength for each the 19 samples (see Table 1)

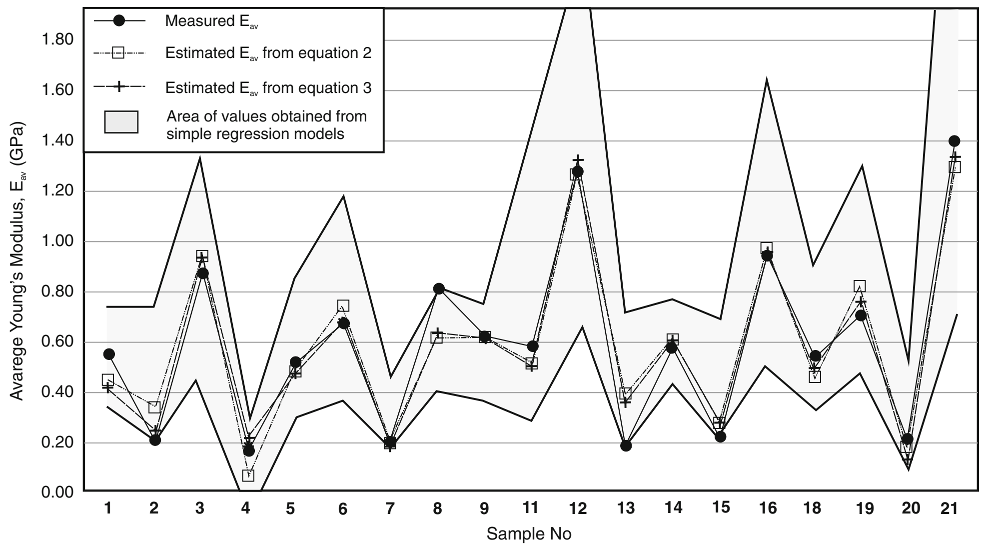

Fig. 13 Comparison of measured and estimated values of the average Young's modulus for the samples (see Table 1)

$V_p + 0.427UW$, $E_{av} = 0.944 + 5.899 \times 10^{-4}\ V_p - 3.17 \times 10^{-2} n$ and $E_{av} = 2.201 + 6.244 \times 10^{-4}\ V_p - 4.30 \times 10^{-2}\ n - 1.09 \times 10^{-3}\ I_{d2}$ are more useful and practical for rock mechanics investigations. These equations are likely to be applicable for other caliche deposits with a similar mineralogical structure to those reported in this study. However, it is strongly recommended that they are not assumed to applicable to all caliche deposits.

Acknowledgments This study was supported by TÜBİTAK (Project No: 104Y189). The authors would also like to thank the Çukurova University Scientific Research Project Unit for providing financial support (Projects No: MMF-2004BAP-11 and MMF-2004D-19).

References

Aggistalis G, Alivizatos A, Stamoulis D, Stournaras G (1996) Correlating uniaxial compressive strength with Schmidt hammer rebound number, point load index, Young's modulus, and mineralogy of gabbros and basalts (Northern Greece). Bull Eng Geol 54:3–11

Aufmuth ER (1973) A systematic determination of engineering criteria for rocks. Bull Assoc Eng Geol 11:235–245

Beverly BE, Schoenwolf DA, Brierly GS (1979) Correlations of rocks index values with engineering properties and the classification of intact rocks

Bieniawski ZT (1974) Estimating the strength of rock materials. J S Afr Inst Min Metall 74:312–320

Çobanoğlu I, Bozdağ Ş, Kumsar H (2008) Microstructural, geochemical and geomechanical properties of caliche deposits from the Adana Basin, Turkey. Bull Eng Geol Environ (in press)

Davis JC (1986) Statistics and data analysis in geology. Wiley, Canada

Deere DU, Miller RP (1966) Engineering classification and index properties for intact rocks. Tech Rep Air Force Weapons Lab, New Mexico, no AFNL-TR, pp 65–116

Dinçer İ, Acar A, Çobanoğlu İ, Uras Y (2004) Correlation between Schmidt hardness, uniaxial compressive strength and Young's modulus for andesites, basalts and tuffs. Bull Eng Geol Environ 63:141–148

Fahy MP, Guccione MJ (1979) Estimating strength of sandstone using petrographic thin-section data. Bull Assoc Eng Geol 16:467–485

Ghose AK, Chakraborti S (1986) Empirical strength indices of Indian coals–an investigation. In: Proceedings of 27th US symposium on rock mechanics, Balkema, Rotherdam, pp 59–61

Goudie PA, Pye K (1983) Chemical sediments and geomorphology. Academic Press, London, pp 93–131

Gökçeoğlu C (1996) Schmidt sertlik çekici kullanılarak tahmin edilen tek eksenli basınç dayanımı verilerinin güvenirliği üzerine bir değerlendirme (in Turkish). Jeol Müh Dergisi 48:78–81

Gunsallus KL, Kulhawy FHA (1984) Comparative evaluation of rock strength measures. Int J Rock Mech Min Sci Geomech Abstr 21:233–248

Haramy KY, DeMarco MJ (1985) Use of Schmidt hammer for rock and coal testing. In: Proceedings of 26th US symposium on rock mechanics, 26–28 June, Rapid City, pp 549–555

Horta JC (1980) Calcrete, gypcrete and soil classification in Algeria. Eng Geol 15:15–52

IAEG (1979) Report of the commission on engineering geological mapping. Bull IAEG 19:364–371

ISRM (International Society for Rock Mechanics) (1978a) Commission on Standardization of Laboratory and Field results. Suggested Methods for Determining Hardness and Abrasiveness of Rocks. Int J Rock Mech Min Sci Geomech Abstr 15:89–97

ISRM (International Society for Rock Mechanics) (1978b) Suggested Methods for Determining Sound Velocity. Int J Rock Mech Min Sci Geomech Abstr 15:53–58

ISRM (International Society for Rock Mechanics) (1979) Commission on Standardization of Laboratory and Field Tests, Suggested Methods for Determining Water Content, Porosity, Density, Absorption and Related Properties and Swelling and Slake Durability Index Properties. Int J Rock Mech Min.Sci 16:148–156

ISRM (International Society for Rock Mechanics) (1981a) Rock Characterization Testing and Monitoring, ISRM Suggested Methods. International Society for Rock Mechanics, 211 pp

ISRM (International Society for Rock Mechanics) (1981b) Suggested Methods for Determining Hardness and Abrasiveness of Rocks, part 3. Commission on Standardisation of Laboratory and Field Tests, pp 101–102

ISRM (International Society for Rock Mechanics) (1981c) Suggested Methods for Determining the Uniaxial Compressive Strength and Deformability of Rock Materials. International society for rock mech. Commission on Standardisation of Laboratory and Field Tests, pp 111–116

ISRM (International Society for Rock Mechanics) (1985) Suggested Methods for Determining Point-load Strength. Int J Rock Mech Min Sci 22:53–60

Kahraman S (1996) Basınç direnci tahmininde schmidt ve nokta yük indeksi kullanmanın güvenirliği. In: Korkmaz ve S, Akçay M (eds) KTÜ Jeoloji Mühendisliği Bölümü 30. Yıl Sempozyumu Bildiriler Kitabı, Trabzon, pp 362–369 (in Turkish)

Kahraman S (2001) Evaluation of simple methods for assessing the uniaxial compressive strength of rock. Int J Rock Mech Mining Sci 38:981–994

Kapur S, Yaman S, Gökçen SL, Yetiş C (1993) Soil stratigraphy and Quaternary caliche in the Misis area of the Adana basin, southern Turkey. Catena 20:431–445

Karakuş M, Kumral M, Kılıç O (2004) Predicting elastic properties of intact rocks from index tests using multiple regression modeling (Technical note). Int J Rock Mech Mining Sci 42:323–330

Katz O, Reches Z, Roegiers JC (2000) Evaluation of mechanical rock properties using a Schmidt hammer. Tech Note Int J Rock Mech Min Sci 37:723–728

Kindybinski A (1980) Bursting liability indices of coal. Int J Rock Mech Min Sci Geomech Abstr 17:167–161

Koncagül EC, Santi Paul M (1999) Predicting the unconfined compressive strength of the Breathitt shale using slake durability, Shore hardness and rock structural properties. Int J Rock Mech Mining Sci 36:139–153

Miller RP (1965) Engneering classification and index properties for intact rock. PhD Thesis, University of Illinois

O'Rourke JE (1989) Rock index properties for geo-engineering in underground development. Min Eng 106–110

Sachpazis CI (1990) Correlating Schmidt hammer rebound number with compressive strength and Young's modulus of carbonate rocks. Bull Int Assoc Eng Geol 42:75–83

Shakoor A, Bonelli RE (1991) Relationship between petrographic characteristics, engineering index properties and mechanical properties of selected sandstones. Bull Assoc Eng Geol 28:55–71

Shorey PR, Barat D, Das MN, Mukherjee KP, Singh B (1984) Schmidt hammer rebound data for estimation of large scale in-situ coal strength (Tech Note). Int J Rock Mech Min Sci Geomech Abstr 21:39–42

Singh RN, Hassani FP, Elkington Pas (1983) The application of strength and deformation index testing to the stability assessment of coal measures excavations. In: Proceedings of 24th US symposium on rock mechanics, Texas A&M Univ, AEG, pp 599–609

Wright VP, Tucker ME (1991) Calcretes. IAS Repr Ser, vol 2. Blackwell, Oxford, 352 pp

Xu S, Grasso P, Mahtab A (1990) Use of Schmidt hammer for estimating mechanical properties of weak rock. 6th Int IAEG Congress. Balkema, Rotterdam, pp 511–519

Yaşar E, Erdoğan Y (2004a) Correlating sound velocity with the density, compressive strength and Young's modulus of carbonate rocks (Technical Note). Int J Rock Mech Mining Sci 41:871–875

Yaşar E, Erdoğan Y (2004b) Estimation of rock physicomechanical properties using hardness methods. Eng Geol 71:281–288

Yılmaz I, Sendir H (2002) Correlation of Schmidt hammer rebound number with unconfined compressive strength and Young's modulus in gypsum from Sivas (Turkey). Eng Geol 66:211–219

Yılmazer I, Smith I (1992) Yumuşakken ve sertken seviyelerinden oluşan kalişin jeolojik ve jeoteknik özellikleri (in Turkish). Türkiye jeoloji kurultayı Bülteni S7:145–152

Zorlu K, Kasapoğlu KE (2004) Adana yöresindeki kalişlerde iç yapı çökme potansiyelinin tahminine yönelik görgül bir yaklaşım (in Turkish). Hacettepe Üniversitesi Yerbilimleri Dergisi 29:133–141